Petrographic Characterization, Diagenetic Implications and its Effects on the Carbonate Reservoir Quality of the Kareem and Rudeis Formations, Zeit Bay Oil Field, Gulf of Suez, Egypt

Elshahat, O.R.[1], El-Shayeb, H.[2], Abd El-Gawad, E.[1], El-Desouki, H[2] and Haddad, I.[3]

[1]Geology Department, Faculty of Science, Al-Azhar University
[2]Geology Department, Faculty of Science, Menoufia University
[3]Egyptian General Petroleum Corporation
osamaramzy80@yahoo.com

Abstract: The Lower- Middle Miocene (Upper Aquitanian-Serravallian) Kareem and Rudeis formations of the Gulf of Suez are composed of mixed siliciclastic/carbonate rocks. Eight carbonate microfacies are recognized and described including mudstone, wackestone- packstone, packstone- grainstone and boundstone. The observed post-depositional changes in the studied rock units include (approximately in a paragenetic sequence): cementation, recrystallization, dolomitization, pressure solution, dedolomitization and dissolution and fillings. Petrographical studies of the Kareem and Rudeis formations revealed the presence of different types of secondary porosity which include: intra-intercrystalline, vuggy, fractures and channel porosity. Dissolution dolomitization and dedolomitization were improved the reservoir quality, and generated secondary porosity such micro-inter-crystalline and vuggular, porosity. While cementation had most effect on decline the porosity and permeability in the Kareem and Rudeis reservoir.

1. Introduction

Zeit Bay Oil field is located in the southwest offshore margin of the Gulf of Suez, in a shallow water depth (water is of up to 65 ft depth) just east of Ras El Bahar Peninsula between Longitudes $33^0 32^'$ and $33^0 37^'$E and Latitudes $27^0 42^'$ and $27^0 47^'$ N (Fig. 1). The field is located 65 km north of Hurghada, 85 km south of Ras Gharib and 12 km north of the abandoned Gemsa oil field. The Zeit Bay field is a NW-SE-trending structure containing clastic and carbonate rocks overlying a tilted block of granitic basement rocks. Many works concerning tectonic, structural and sedimentlogical studies of the Gulf of Suez were published (e.g., Abdel Gawad, 1970; Chenet and Letouzey, 1983 and Meshrif, 1990). The present work aims to describing the microfacies in the carbonate rocks of the Kareem and Rudeis formations and their diagenetic aspects also their effects on the reservoir quality in the Zeit Bay oil field which have not been described in detail before.

Geologic Settings

Structure and Tectonism

The Gulf of Suez occupies the northern extension of the Red Sea rift (Said, 1962) and is separated from it by the Aqaba transform faults. The rifting that was caused by tensional stresses commenced in the pre-Miocene, with the maximum tectonic subsidence, accompanied by magmatic events, (Gandino et al., 1990). The timing of rifting was dated as Late Oligocene to Early Miocene (Fichera et al., 1992).

The opening of both the red sea and the Suez rift resulted by the extension in (Afro-Arabian plate) leading to the separation of the African, Sinai and Arabian plate during the late Eocene to Oligocene (Moustafa, 1997).
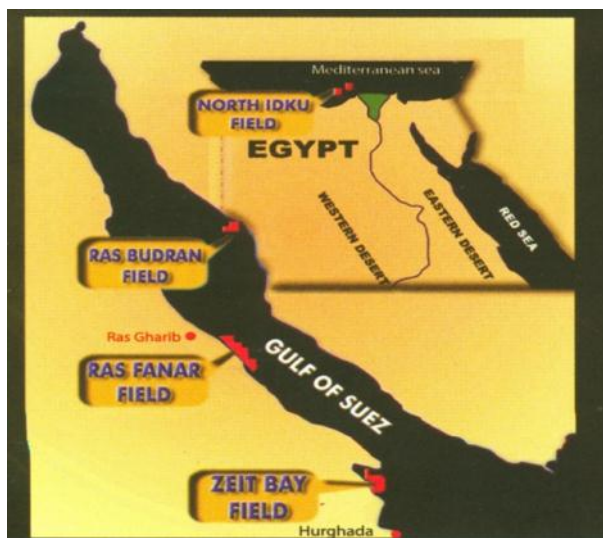

Fig. 1: Location map of the Zeit Bay Oil Field.

Generally, the Gulf of Suez is subdivided into three structural provinces according to the dominant structural dip of the sedimentary sequences (Moustafa,

1976), the northern Araba dip province (SW dips), the central Belayim dip province (NE dips), and the southern Amal-Zeit dip province (SW dips) (Abd El-Naby et al., 2010). These provinces are separated by two NE-trending accommodation zones: the Galala-Abu Zenima Accommodation zone (GAZAZ) in the north and the Morgan Accommodation zone (MAZ) in the south.

Structurally, the Zeit Bay field is interpreted as a NW–SE basement relief like anticlinal feature. This anticlinal feature is, however, dissected into several fault block panels by two main fault systems. A set of NW–SE trending faults affecting the western and eastern flanks. Another set of WNW/E-SE trending fault system affecting the northeast flank (Khaled et al., 2009).

Stratigraphic settings of the Gulf of Suez

The lithostratigraphic units in the Gulf of Suez were subdivided into three major sequences related to the Miocene rifting event: a prerift succession (pre-Miocene or Paleozoic– Eocene), a synrift succession (Oligocene–Miocene), and a postrift succession (post-Miocene or Pliocene–Holocene) (Fig. 2). These units vary in lithology, thickness, areal distribution, depositional environment, and hydrocarbon importance (Alsharhan and Salah, 1997).

Stratigraphic settings of the Zeit bay oil field

The stratigraphic column of the Zeit bay field includes the rock units ranging in age from Early Carboniferous to Post Miocene normally encountered in the Gulf of Suez basin. The Miocene in the Gulf of Suez is regionally classified into two main groups: the Lower Miocene Gharandal Group and the Middle Miocene Ras Malaab or Evaporite Group (Egyptian General Petroleum Corporation (EGPC, 1964 and Gawad et al., 1986).

The Gharandal Group comprises (from base to top) the Nukhul, Rudeis and Kareem formations. These Miocene rocks are unconformably underlain by Paleozoic to Mesozoic Sandstone of Nubia facies which cover unconformably the Precambrian basement rocks (Fig.2).
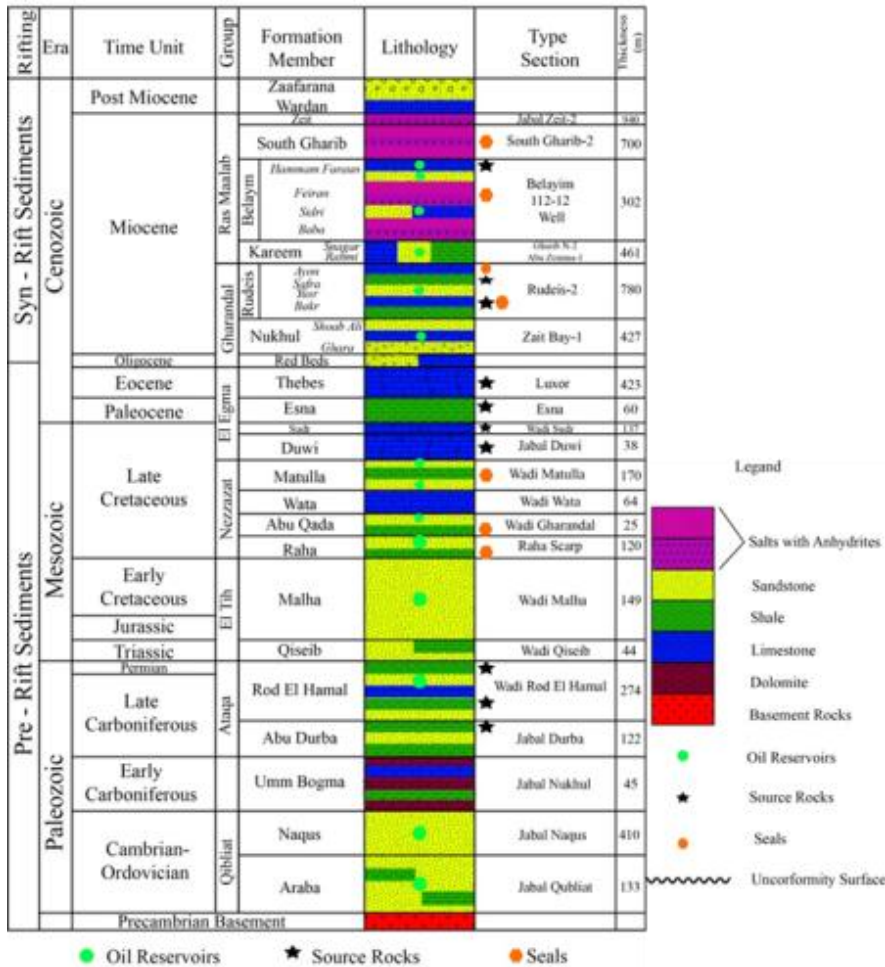

Fig. 2: General stratigraphic succession of Gulf of Suez (modified from Alsharhan and Salah 1997).

The Kareem Formation was introduced by the EGPC Stratigraphic Committee (1964) to describe the uppermost rock unit of the Lower to Middle Miocene Gharandal Group. The Kareem Formation is bounded by two unconformities separated it from the underlying open marine Rudeis Formation and the overlying Belayim Formation that was deposited in greatly fluctuating depositional environments.

The EGPC committee (1964) divided the Kareem Formation into two unconformably members. The lower member is known as the Rahmi Member which is made up of thin beds of anhydrite intercalated with sandstone, shale and carbonate rocks. The depositional setting of the Rahmi Member was shallow, partly open marine, with lagoonal conditions. The upper member is termed Shagar Member that consists of interbedded shale, limestone and sandstone. It was deposited in deep inner to shallow outer sublittoral setting. The boundary two members are defined by the first appearance of anhydrite (Tewfik et al., 1992).

The Early Middle Miocene (Langhian–Serravallian) age was assigned to the Kareem Formation by El Beialy and Ali (2002) and El Beialy et al. (2005). The thickness of the Kareem Formation is up to 1400 ft. (Tewfik et al., 1992).

The Rudeis Formation conformably overlies the Nukhul Formation and is disconformably overlain by Kareem Formation. It varies greatly in lithology, thickness and depositional setting, in response to their irregular paleo-relief over which sedimentation took place (Tewfik et al., 1992). The Rudeis Formation consists mainly of shale and limestones that are interbedded with sandstone. The Rudeis Formation has variable thickness ranging from 200-500 ft.

The Rudeis Formation was subdivided into four members which are (from base to top): Bakr, Yusr, Safra and Ayun members. Several operating oil companies have further subdivided the Rudeis Formation. Most companies have subdivided the Rudeis Formation into two units (lower and upper). The lower unit (Late Aquitanian) is made up of mixed siliciclastic rocks (light brown calcareous shale and highly calcareous sandstone, partially glauconitic) and few streaks of limestone (Samir, 2012). The upper unit (Burdigalian) consists mainly of light brown calcareous shale, partially glauconitic and rich in planktonic and benthonic foraminifera, argiliceous limestone and gritty sandstone. The depositional environment of the Rudeis Formation is alternating between shallow and deep marine (Balduzzi et al., 1978; Said, 1990; El Beialy and Ali 2002 and Amgad, 2011).
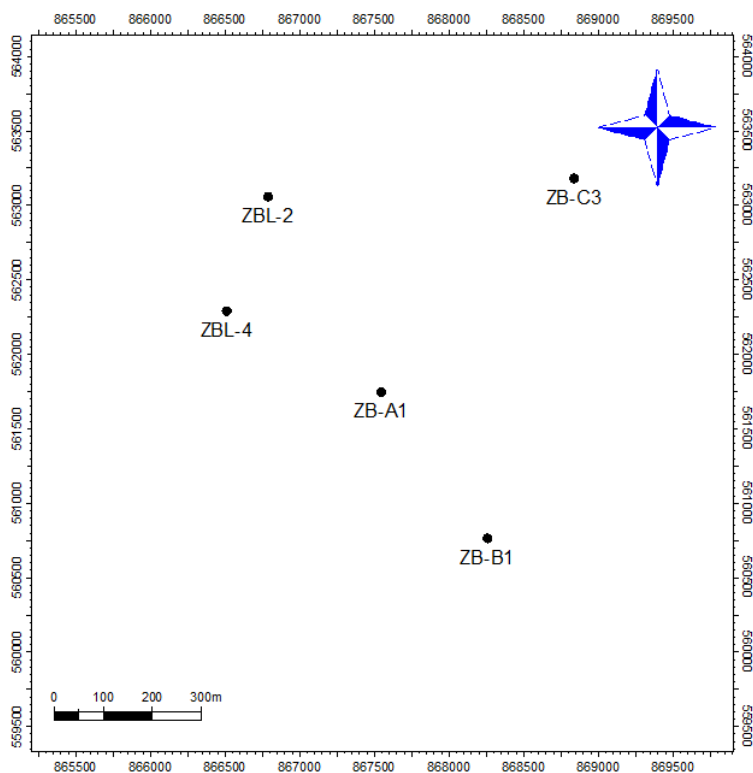

Fig. 3: Location map of the studied wells in the Zeit Bay oil Field.

Petrographical studies
Microfacies analysis

This study covers the petrographical investigation of 22 carbonate samples of the core intervals taken in the Kareem and Rudeis formations (Table 1) in wells ZB-A$_1$, ZB-B$_1$, ZB-L$_2$, ZB-L$_4$ and ZB-C$_3$ in Zeit Bay oil field (Fig. 3). The petrographical analysis of these samples led to the recognition of eight (8) carbonate microfacies associations occur in the studied rock units (Kareem and Rudeis formations). The classification schemes by Folk (1962) and Dunham (1962) were used in the petrographic study. The following is a petrographic description of these microfacies types:

Table 1: Showing conventional and side well cores.

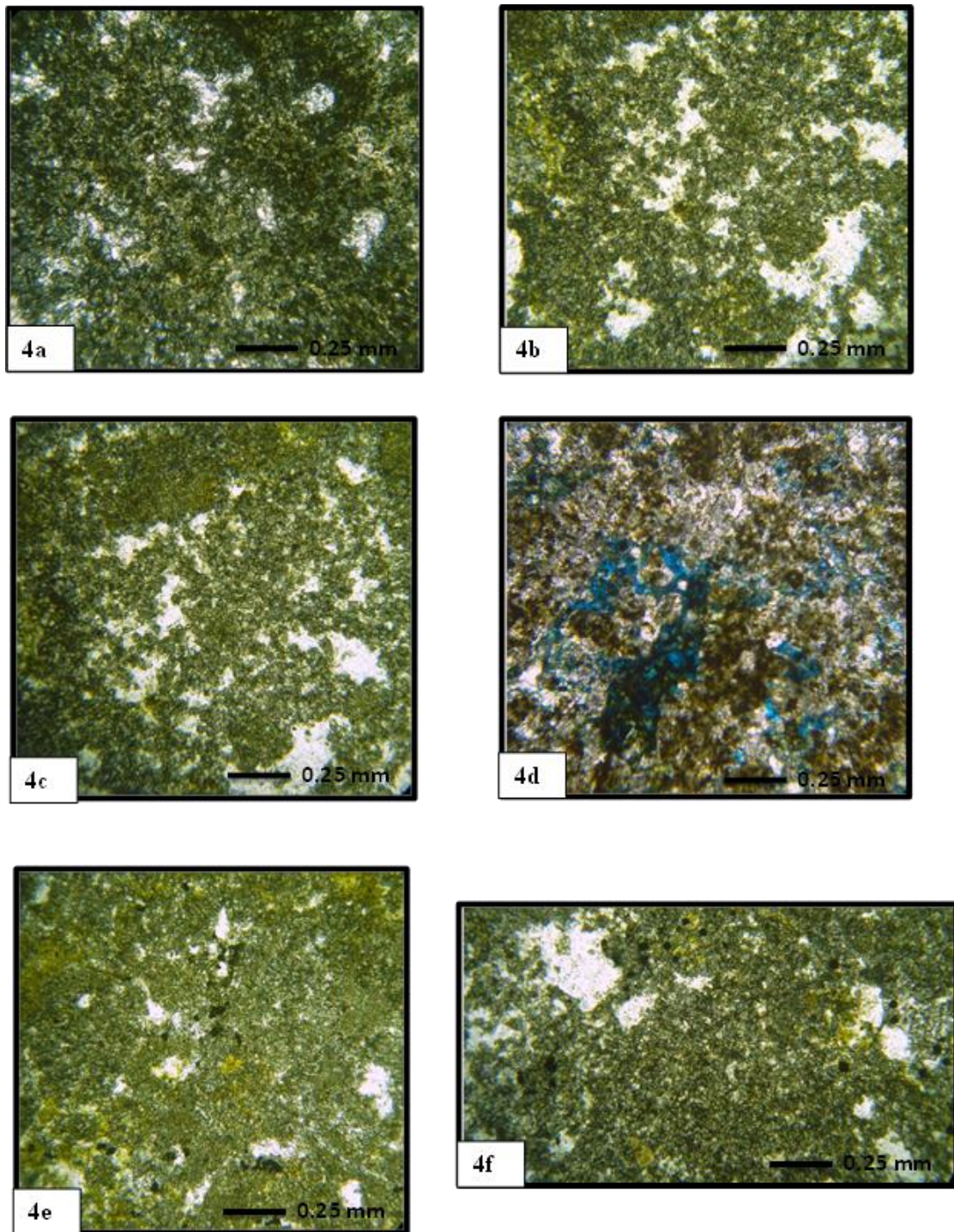| Well Name	ZB-B$_1$				
Formation Tops	Top MD	Core No.	Interval	Rec.	No. of thin sections
Belayim	3954'				
Kareem and Rudeis	4050'	1	4600'-4630'	30'	1
		2	4630'-4660'	30'	1
		3	4660'-4690'	28'	1
Basal Miocene Sandstone	4655'				
ZB-C$_3$					
Formation Tops	Top MD	Core No.	Interval	Rec.	No. of thin sections
Belayim	4128'				
Kareem and Rudeis	5042'	1	5345'-5384'	41'	1
		2	5384'-5430'	42'	1
		3	5430'-5490'	13'	1
		4	5490'-5516'	7'	1
		5	5516'-5518'	51'	1
		6	5518'-5519'	56'	1
Basal Miocene SD	5520'				
ZB-L$_2$					
Formation Tops	Top MD	Core No.	Interval	Rec.	No. of thin sections
Belayim	4512'				
Kareem and Rudeis	4695'	1	5163'-5194'	31'	
		2	5287'-5309'	22'	2
		3	5309'-5324'	15'	2
Basal Miocene Sandstone	5314'				
ZB-A$_1$					
Formation Tops	Top MD	Core No.	Interval	Rec.	No. of thin sections
Belayim	4010'				
Kareem and Rudeis	4310'	1	4328'-4369'	41'	1
		2	4372'-4414'	42'	1
		3	4418'-4431'	13'	1
		4	4433'-4441'	7'	1
		5	4442'-4492'	51'	1
		6	4493'-4549'	56'	1
		7	4549'-4610'	61'	1
		8	4610'-4671'	61'	1
		9	4671'-4744'	73'	1
Basal Miocene Sandstone	4719'				
ZB-L$_4$					
Formation Tops	Top MD	Core No.	Interval	Rec.	No. of thin sections
Belayim	4800'				
Kareem and Rudeis	5294'	1	5327'-5379'	52'	1
		2	5379'-5439'	60'	1
		3	5439'-5499'	60'	1
		4	5499'-5550'	51'	1
Basal Miocene Sandstone	5550'				

Fig.4: The carbonate mudstone (Dolosparite) microfacies:
a, b, c and d). Small to medium, subhedral- euhedral dolomite crystals. e and f): showing the presence of hydrocarbon residues which filling the space between dolomite crystals.
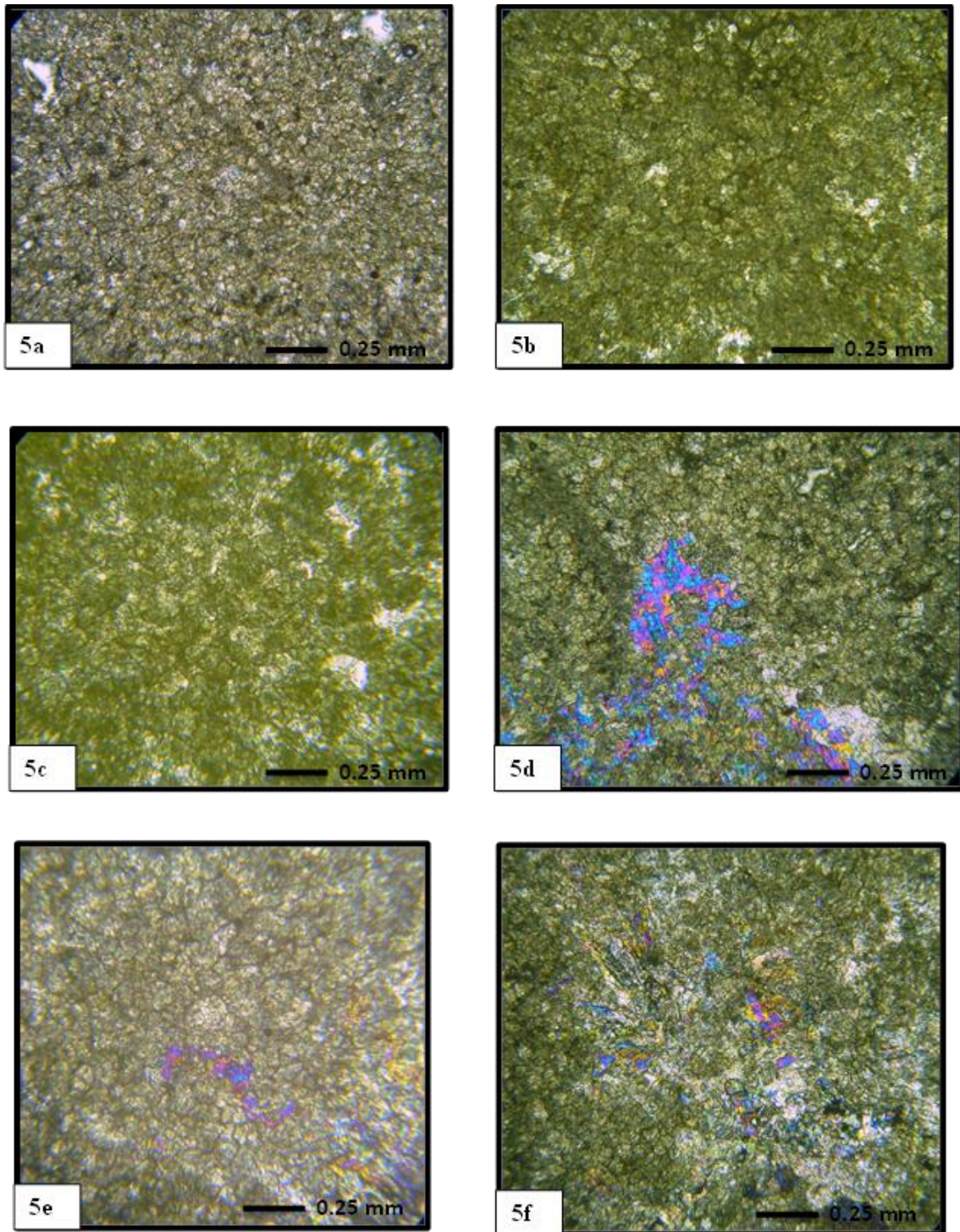
Fig.5: The carbonate mudstone (Anhydritic algal dolosparite) microfacies:
a, b and c) Very fine to fine, clear, un zoned euhedral- subhedral dolomite rhombs ground mass.
d, e and f)   Anhydrite crystals are present in the form of large crystals or filling the fractures and
pores, anhydrite crystals show rectangular cleavage.
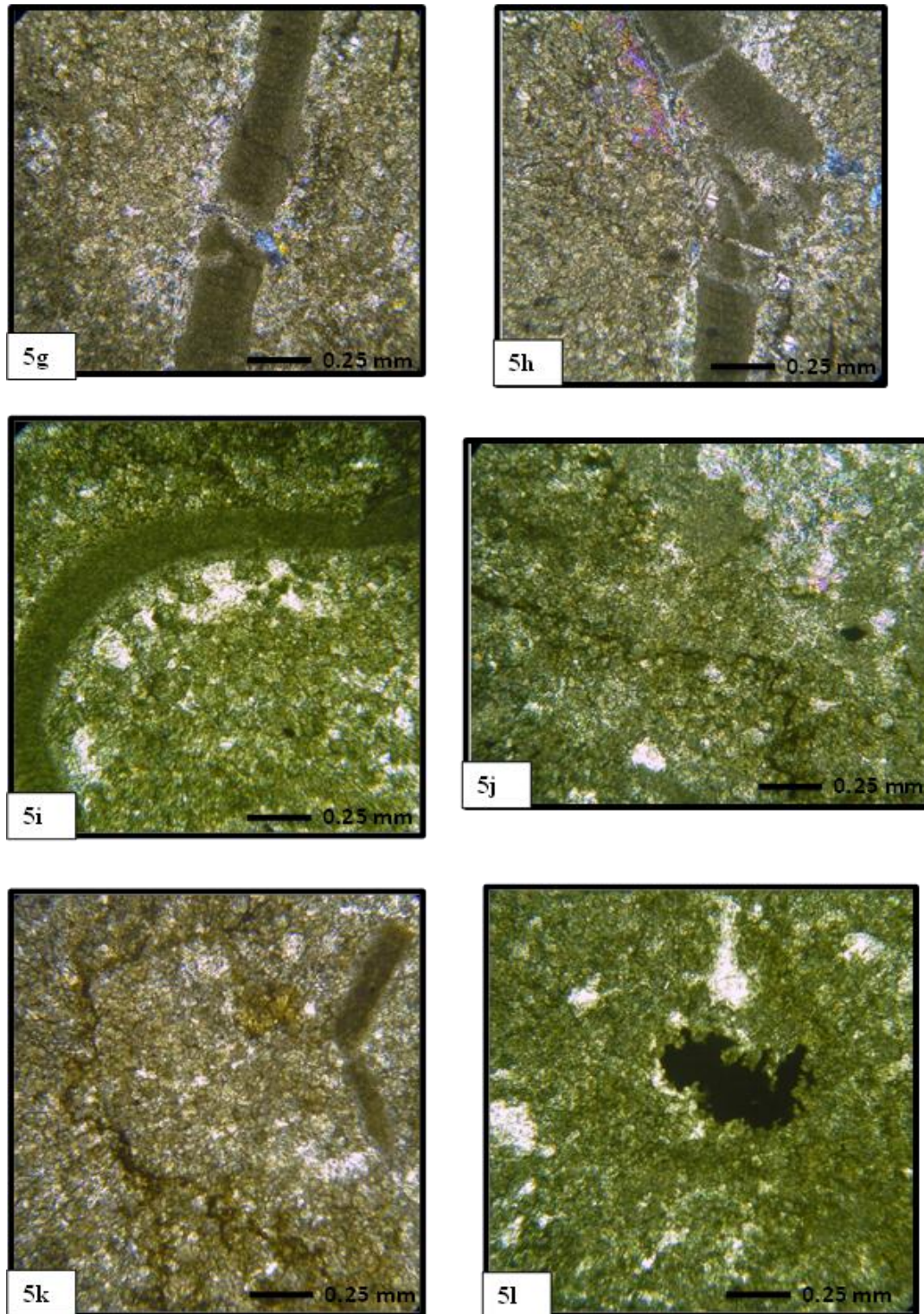
Fig.5: The carbonate mudstone (Anhydritic algal dolosparite) microfacies:
g, h and i) Micritized calcareous red algal shells, (less than 10%). j and k): A jagged, columnar surface (stylolite fractures,), filled with insoluble minerals (or iron oxides) or hydrocarbon residues. l): Hydrocarbon residues which accumulated and filling the space between dolomite crystals.

Carbonate mudstones

This mud supported microfacies is represented by dolosparite, anhydritic algal dolosparite, sandy dolosparite, sandy algal dolosparite and anhydritic dolosparite.

The dolosparite microfacies (Fig. 4) is of limited distribution in the studied wells. Samples were obtained from wells ZB-A_1, core 1, 2 and 3 at depths 4328 ft., 4418 ft. and 4433 ft. respectively and ZB-L_4, core 1 at depth 5327 ft.

This microfacies is composed entirely of dolomitic limestone of small, subhedral- euhedral shape crystals (Fig. 4a, b, c and d), the undolomitized limestone surrounding the dolomite shows patchy texture or relicts of micrite. Very fine quartz crystals (>2 %) are embedded in micrite matrix, some of calcareous red algal shell fragments (>2 %) are filled with sparite of different size (aggrading neomorphism with relics of micrite) and have micritic edges.

There are hydrocarbon residues which stain the surrounding micrite and fill the space between the microsparite crystals and microfractures (Figs. 4e, and f). The detected iron oxide as dispersed patches and cement in some samples reflects an oxidation condition accomplished with humid and arid conditions, resulting in deposition of iron oxide from pore water.

Small poikilitic anhydrite crystals with high relief and strong birefringence are present. Medium to large grains (intraclasts) with a smooth, rather than botryoidal, external form are bounded by micritic material which is completely envelopes them. These particles are probably reworked grains.

Dolosparite microfacies indicates deposition in the deeper part of the neritic zone, far from landmass with alkaline medium, normal salinity, clear, calm and warm water (Abdel-Hafez, 1987).

The anhydritic algal dolosparite microfacies (Fig. 5) is the major carbonate microfacies in the studied samples. It occurs in ten samples and is distributed in the studied wells as the following: well ZB-A_1 (core 6, 7 and 8 at depths 4439 ft., 4550 ft. and 4611 ft., respectively), well ZB-L_4 (core 2, 3, 4 and 5 at depths 5379 ft., 5439 ft., 5499 ft. and 5557 ft., respectively) and well ZB-B_1 (core 1, 2 and 3 at depths 4600 ft., 4630 ft. and 4660 ft., respectively).

This microfacies is composed mainly of fine to medium, clear, un zoned euhedral- subhedral dolomite rhombs ground mass (Figs. 5a, b and c).

Anhydrite crystals (up to 45%) are present in the form of large crystals or filling the fractures and pores. They show rectangular cleavage (Figs. 5d, e and f). The anhydrite crystals are characterized by high relief, strong birefringence, bladed in the form of laths with radiation habit showing the bright second interference colors. Rare gypsum crystals with low relief, weak

birefringence and first-order pale grey color are present.

Some calcareous red algal shells and shell fragments (micritized), less than 10% are present (Figs. 5g, h and i). A jagged, columnar surface (stylolite fractures), hydrocarbon residues (or iron oxides) are seen throughout these stylolitic pore spaces (Fig. 5j, and k). Fracture porosity is the main type of second porosity found in the studied samples. Hydrocarbon residues which filling the space between dolomite crystals (Fig. 5l).

The sandy dolosparite microfacies (Fig 6) has a restricted distribution in the studied wells. It was recorded in wells ZB-C_3, core 2 at depth 5384 ft., core 4 at depth 5475 ft. and ZB-L_2, core 3at depth 5309 ft.

The framework of this microfacies is composed essentially of mosaics of dolosparite rhombs. The rhombs are fine, un zoned, subhedral crystals, with intercrystalline pore spaces. Scattered detrital quartz grains (up to 20 %) occur. These quartz grains are subround to subangular highly fractured, fine - to coarse - grained sand with normal and wave extinction (Fig. 6a, b and c). Some fractures are filled with hydrocarbons. Calcareous red algal shells (>4 %) occur (Fig. 6d). Channel, fracture, vug and intercrystal are the main type of porosity found in this microfacies.

The sandy algal dolosparite microfacies (Fig. 7) have a very limited distribution. It occurs only in well ZB-L_4, core 6 at depth 5567 ft. The framework is composed essentially of very fine - to fine -, clear, un zoned, euhedral-subhedral dolomite rhombs (Fig. 7a). Scattered detrital quartz grains (10 %) of fine - to coarse - grained sand size, normal and wave extinction, subround to subangular occur (Fig. 7a). Calcareous red algal fragments (20 %) are present (Fig. 7b and c). Hydrocarbons were filling stylolite fractures (Fig. 7d). Widespread development of intragranular (moldic) porosity was observed in this sample.

The anhydritic dolosparite microfacies (Fig. 8) has a very limited distribution and it was recorded only in well ZB-A_1, core 2 at depth 4372 ft. This microfacies is composed of anhydrite crystals with high relief, strong birefringence, bladed, in the form of laths with radiation habit showing the bright second interference colors characteristic of anhydrite. The anhydrite crystals are present in the form of porphyroblast, patches or filling the fractures and pores. The anhydrite crystals show rectangular cleavage (Figs. 8a, b and c). Rare gypsum crystals with low relief, weak birefringence and first-order pale grey color are present. All these components are embedded in fine to medium, centered and un zoned euhedral- subhedral dolomite rhombs. The dark spots seen in the thin section are granules of bituminous carbonate. Channel and fracture porosity are the main type of porosity present in the studied samples.
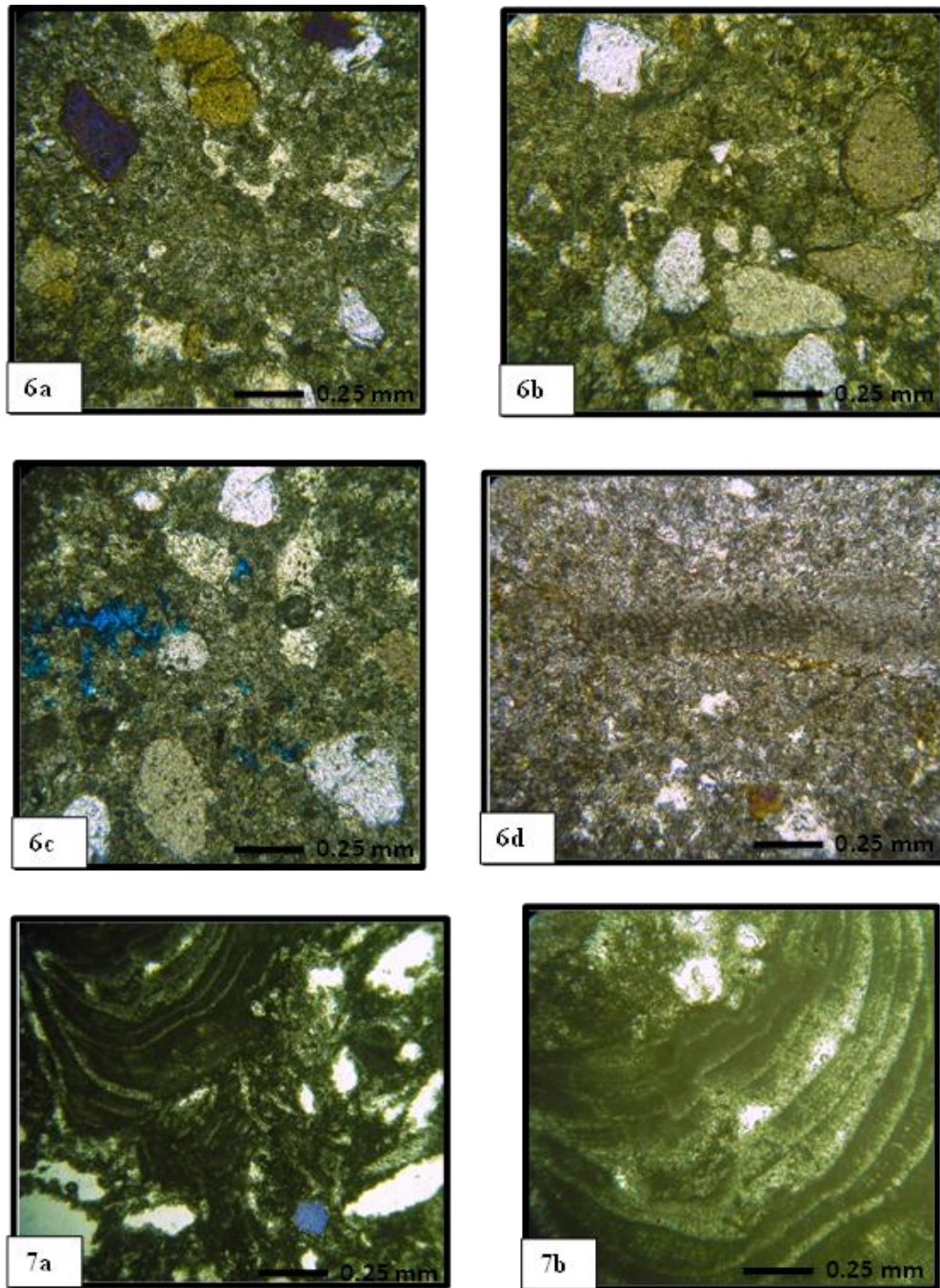
Fig. 6: The carbonate mudstone (Sandy dolosparite) microfacies:
a, b and c): The framework of this microfacies is composed mainly of mosaics, very fine, un zoned, subhedral dolomite rhombs. Scattered detrital quartz grains, (up to 20 %) of fine - to coarse - grained sand size, with normal and wave extinction, subround to subangular and highly fractured. d) Some fractures which are filled with hydrocarbon or iron oxides. Calcareous red algal shells (<4 %), some fractures are filled with hydrocarbon or iron oxides (arrow head).

Fig. 7): The carbonate mudstone (Sandy algal dolosparite) microfacies:
a) Very fine to fine, clear, un zoned, euhedral-subhedral dolosparite rhombs. Quartz grains, (10 %), fine to coarse grained sand size, normal and wave extinction, subrounded to subangular. b) Calcareous red algal shells, (20 %).
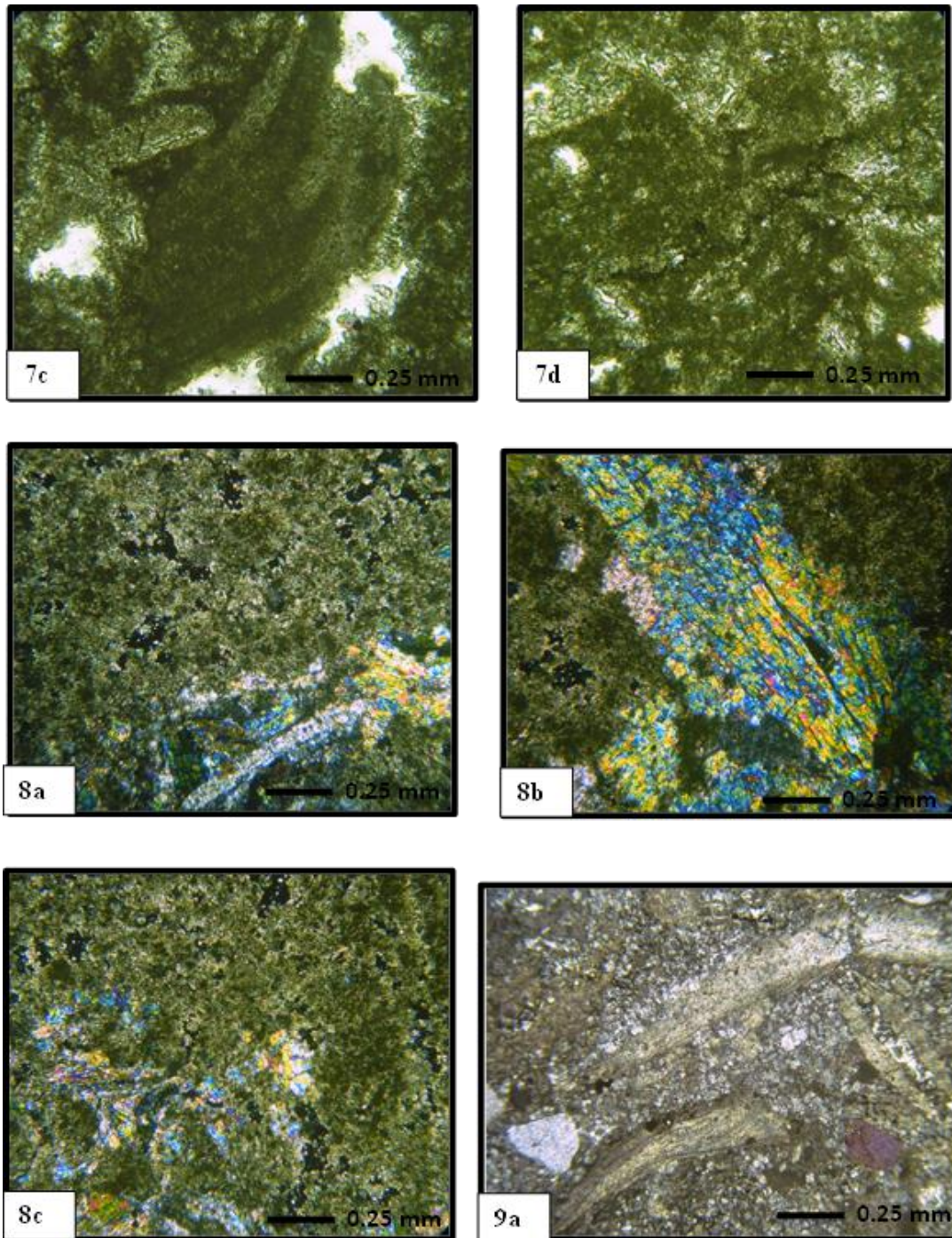
Fig. 7): The carbonate mudstone (Sandy algal dolosparite) microfacies (Continued):
c) Calcareous red algal shells, (15 %). d) Hydrocarbon or iron oxides filling stylolite fracture.

Fig. 8): The carbonate mudstone (Anhydritic dolosparite) microfacies:
a, b and c) This microfacies is composed of anhydrite crystals with high relief, strong birefringence, bladed, in the form of laths with radiation habit showing the bright second interference colors characteristic of anhydrite, the anhydrite crystals are present in the form of porphyroblast, patches or filling the fractures and pores, anhydrite crystals show the rectangular cleavage.

Fig. 9): The Wackestone- packstone (Sandy algal foraminiferal dolomicrite) microfacies:
a) Calcareous algal shells and shell fragment filled entirely with micrite and microsparite, medium to coarse grained, normal and wave extinction, subrounded to subangular detrital quartz grains.

Fig. 9): The Wackestone- packstone (Sandy algal foraminiferal dolomicrite) **microfacies:**
b) Calcareous algal shells and shell fragment filled entirely with micrite and microsparite, medium to coarse grained, normal and wave extinction, subrounded to sub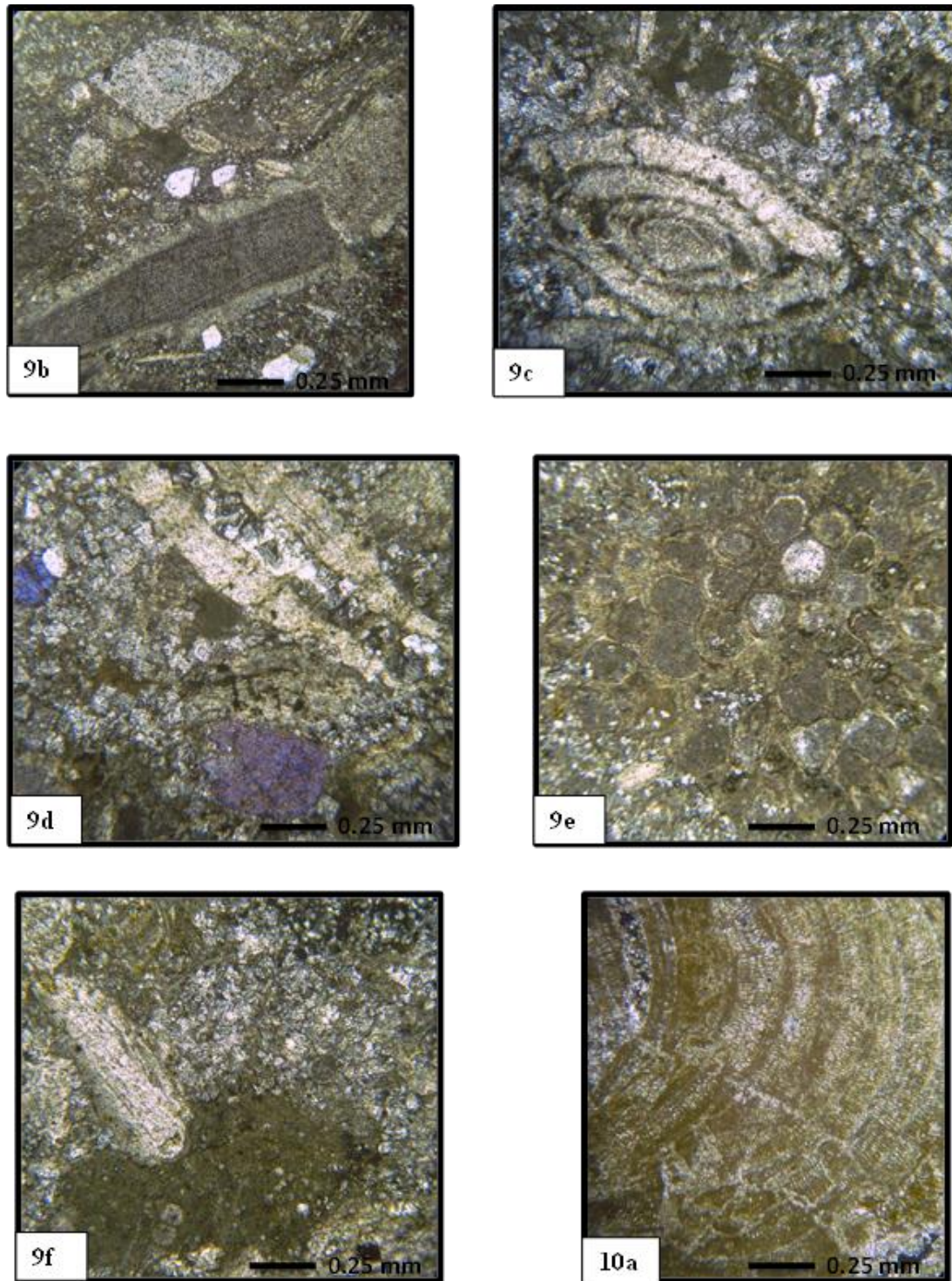angular detrital quartz grains. c and d) *Numulites*, large, thick, coin- or discus-shaped benthic foraminifers filled with sparite. e) Transverse view of a stick-like bryozoans colony, showing the overall rounded shape of the stem, some of these have been infilled with fine sediment but most have sparite calcite cement. Numerous micrite patches are present. f) Gastropods shells, and shell fragments filled with sparite and have micritic wall. The dark spots seen in the thin section are granules of bituminous carbonate.

Fig. 10): the packstone- grainstone (Algal microsparite) microfacies:
a) Composed mainly of calcareous red algal fragments, (25 %), embedded in microsparite calcite cement.

Fig. 10): the packstone- grainstone (Algal microsparite) **microfacies (Continued)**
b): Composed mainly of calcareous red algal fragments, (25 %), embedded in microsparite calcite cement.
Fig. 11): The boundstone (Coralline microsparite) microfacies
a and b) Tabulate coral (with thin wall) embedded in microsparite calcite cement; the internal structure is absent and the pores are filled with sparite cement (non-ferroan calcite). Rare anhydrite patches are present
Fig. 12): Different types of porosity
a and b): Fractures and microfractures porosity.
c) Channel porosity.

Wackestone- packstone

It is represented by a **sandy algal foraminiferal dolosparrymicrite microfacies** (Fig 9). This microfacies occurs only in well ZB-C$_3$, core 1 at depth 5345 ft. The allochems consist of coralline calcareous red algal shells and algal fragments filled entirely with micrite and microsparite (Figs. 9a and b), Nummulites with large, thick, coin- or discus-shaped benthic foraminifers filled with sparite (Figs. 9c, d and f), stick-like bryozoans colony, showing the overall rounded shape of the stem, some of them have been infilled with fine sediment but most have sparite calcite cement (Fig. 9e), gastropods shells and shell fragments filled with sparite and have micritic wall (Fig. 9f). Numerous micrite patches are present (Fig. 9f). The dark spots seen in the thin section are granules of bituminous carbonate (Fig. 9f).

Medium - to coarse - grained sand size, subrounded to subangular detrital quartz grains with normal and wave extinction (Figs. 9a, b and d). All these components are embedded in fine to coarse, clear and un zoned euhedral- subhedral dolomite rhombs. The presence of quartz grains in this microfacies indicating that the depositional environment was continuously receiving abundant detrial materials.

Packstone- grainstone

It is represented by a **algal microsparite**. This microfacies has a very limited distribution and was recorded only in well ZB-A1, core 5 at depth 4442 ft. Algal microsparite microfacies is represented by calcareous red algal fragments (25 %), embedded microsparite calcite cement (Figs. 10a and b).

Boundstone

It is represented by a **coralline microsparite microfacies** which, has a very limited distribution and was recorded only in well ZB-A$_1$, core 2 at depth 4406 ft. it is composed mainly of tabulate coral (with thin wall) embedded in microsparite calcite cement (Figs. 11a and b). The internal structure is absent and the pores are filled with sparite cement (non-ferran calcite). Rare anhydrite patches are present (Figs. 11a and b).

Porosity studies

Porosity description

Many types of pore space were detected during the study of the thin sections of the Kareem/ Rudeis formations of Zeit Bay oil field. A number of classifications of porosity in carbonate rocks have been proposed, but only the Choquette and Pray (1970) scheme has met with widespread acceptance. Thus, it will be the only one described and applied in the present study.

Petrographic observations such as these are essential for the proper understanding of the origin and timing of porosity development or retention in carbonate reservoir rocks. The different types of secondary porosity created, through alteration of a rock, commonly by processes such as dolomitization, dissolution and fracturing) are described as following (Fig. 12):

Fractures and microfractures porosity (Figs. 12a and b):

Fracture porosity commonly constitutes only a few percent of total porosity in carbonate rocks. However, it can have a importance to permeability and hydrocarbon production because it connects pores that may otherwise be largely isolated. Tectonics, compaction and pressure solution are the main reasons forming fractures and microfractures porosity.

Channel porosity (Fig. 12c and d):

The channel porosity (irregular shape) of this large, porous fracture indicates that some solution-enlargement occurred along the fracture.

Vuggy porosity (Figs. 12e, f, g and h):

In the studied samples, the vugs porosity were resulted from dissolution (occurred late in the diagenetic history of this rock) of the dolomite (de-dolomitization) and anhydrite crystals. Vugs porosity is non-fabric selective type where void spaces are formed by post-depositional processes.

Intera-intercrystalline porosity (Figs. 12i, j, k and l):

Intra-intercrystalline porosity is a fabric selective, where pore spaces are located in and between crystals. It is normally associated with dolomites formed in a number of settings ranging from supratidal/sabkha to normal marine sequences (Roehl and choquette, 1986).

Intercrystal porosity is the solution-enlarged intercrystal porosity in a medium-crystalline replacement dolomite. The enormous volume of porosity, coupled with the large and irregular shapes of the intercrystal pores relative to the size of the dolomite rhombs, clearly indicates extensive post-dolomite dissolution of calcite matrix (Peter and Dana, 2003).

Porosity evaluation

Such reservoir rocks have high porosity, but only moderate permeability, because the large moldic pores are connected to each other only through small intercrystalline conduits. The porosity of the Kareem and Rudeis formations is ranging from 17 to 25%, the high porosity value is attributed to the slight increase in the dolomite crystal size which is enhancing both the effective porosity and permeability, and these high porosities are reduced to some limit when anhydrite filling becomes maximum.

Diagenesis and Paragenesis

Diagenesis involves processes that caused the physical, chemical and mineralogical changes in limestone. These processes had occurred since the sediment was deposited and normally it would lead to a more stable condition. Diagenetic processes can enhance, create and/or destroy porosity in carbonate rocks.
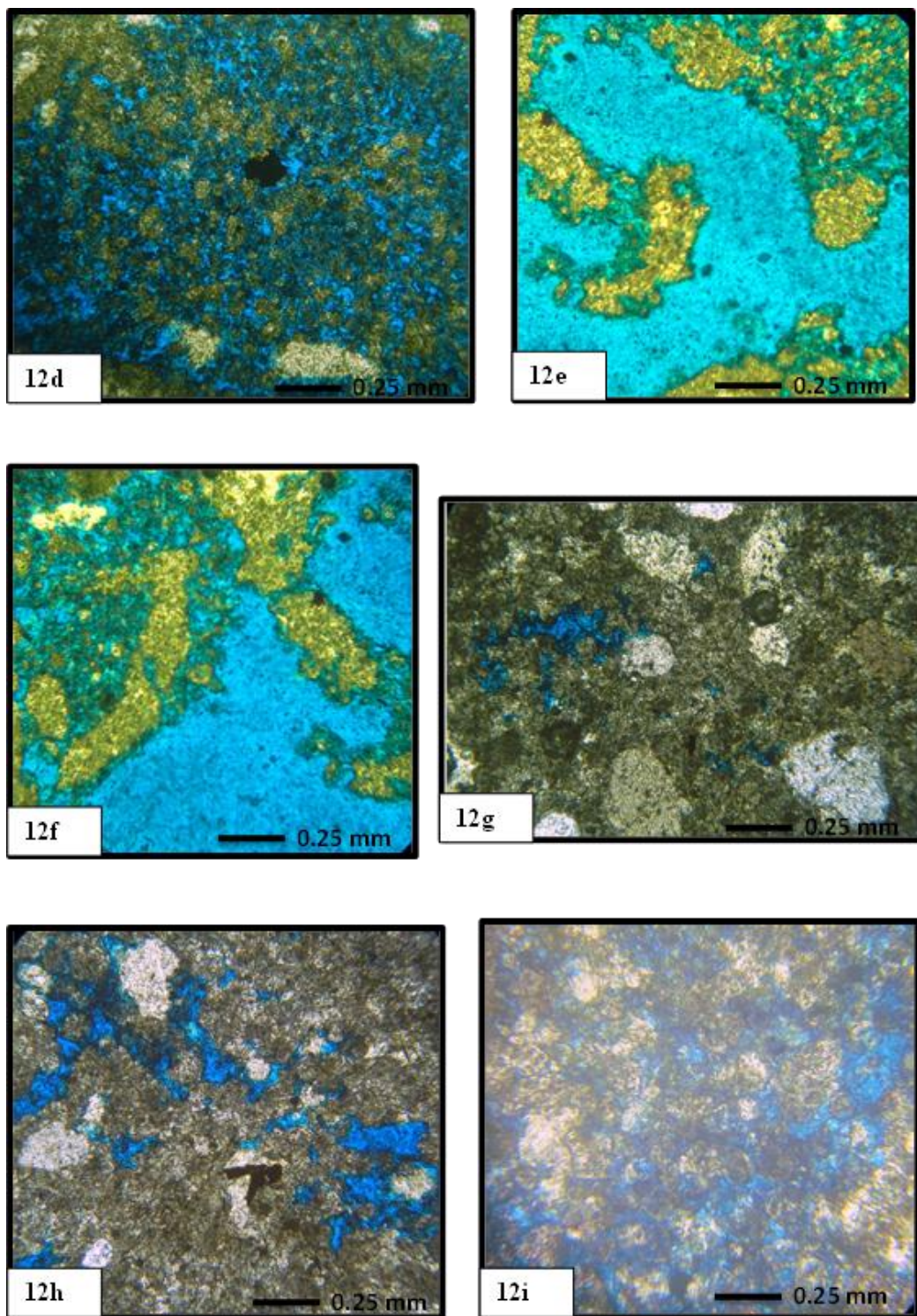
Fig. 12): Different types of porosity
d): Channel porosity.
e, f, g and h): Vuggy porosity.
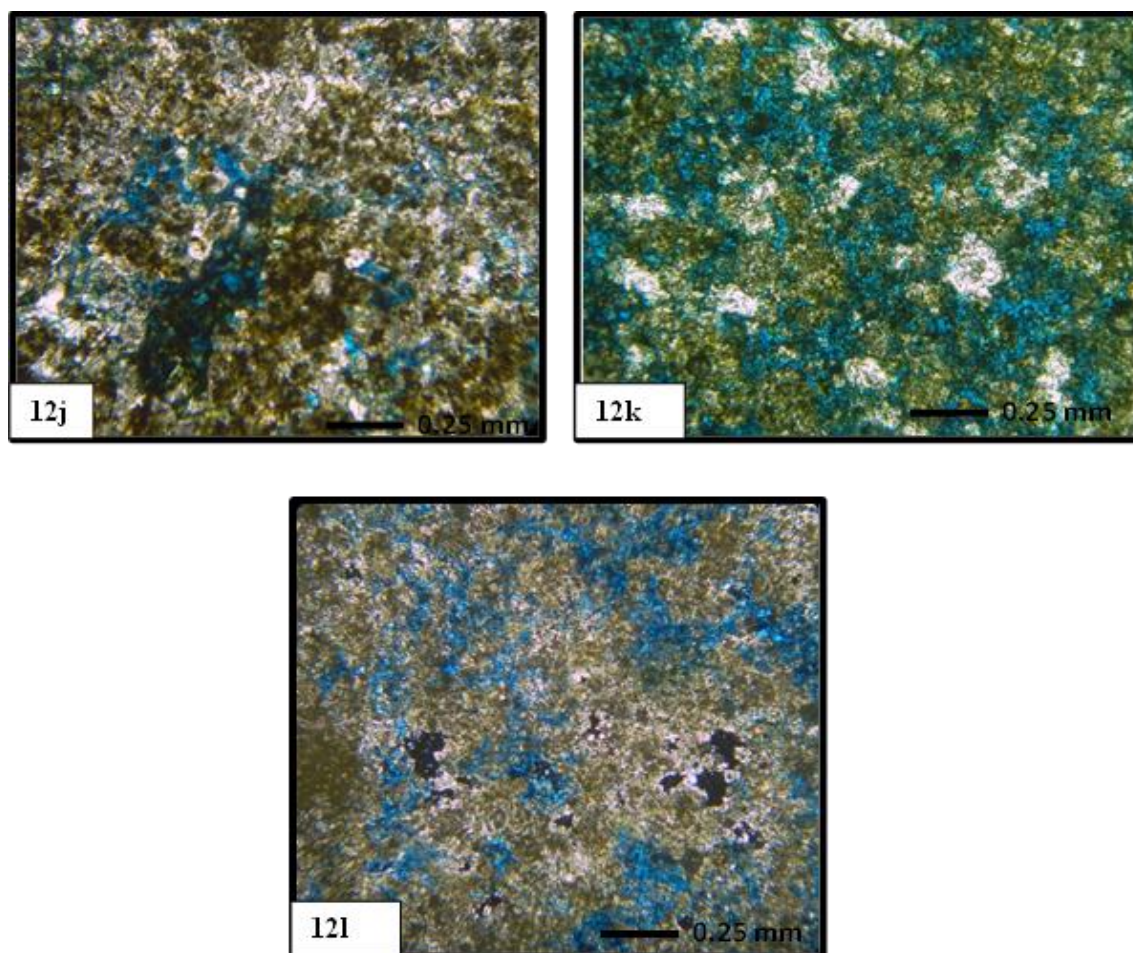i): Intra-intercrystalline porosity.

Fig. 12): Different types of porosity
j, k and l): Intra-intercrystalline porosity.

In essence, several studies signify that the reservoir quality is mainly controlled by the pore-geometry, which, in turn, is mainly determined by various diagenetic processes (Baron et al., 2008; Cerepi et al., 2003; Stentoft et al., 2003 Tucker and Bathurst, 1990). Accordingly, presence or absence of diagenetic imprints along with their type and intensity, play an important role in defining the ultimate reservoir quality and characteristics.

The petrographic examination of the thin sections of the Kareem/ Rudeis carbonate rocks in the Zeit Bay oil Field show that they were subjected to certain effective diagenetic processes. Diagenetic changes include, approximately in a paragenetic sequence, cementation, recrystallization, dolomitization, dedolomitization, pressure solution, dissolution and fillings.

Cementation (9c and 9d):

The early cementation prevents dissolution of the preserved original biogenic content. Thus, the biogenic content may be regarded as retaining a memory of the prediagenetic sediment (El- Albani et al., 2001).

In the studied samples, the cement materials of the investigated rock units are mainly calcium carbonate in the form of sparry calcite filling some skeletal grains and microfractures.

The cementation process is probably attributed to turbulent bottom current and pumping of $CaCO_3$ supersaturated sea water through the sediments in the shallow marine environments of deposition (Tucker, 1981). The cementation process is a major factor that controlling (reducing) the porosity and permeability.

Recrystallization (Figs. 9b, 9e and 9f):

The term recrystallization has been used for a number of processes that cause change in crystal or grain size. Predominantly on enlargement and occasionally a reduction in size without change in chemical alteration except for change in isotopes and trace element concentration.

Rapson - McGaugan (1970) concluded that the recrystallization process takes place in sediment as a result of crystal reorganization due to increase in compactive pressure and crystal reorganization towards stability due to normal aging. Folk (1974) believed that neomorphism of lime mud to microspar, pseudospar and the formation of sparry calcite are related to loss of MgO either by seizure of the Mg by clay minerals or adsorption on the clay, then micritic calcite is free to grow into microspar.

The matrix of the studied carbonates was subjected to recrystallization and changed to dolosparite (with remnant of micrite). It is important to say that the recrystallization process causes a remarkable increases in porosity as a development to the intercrystalline pore space.

Dolomitization (Figs. 4d, 4b, 4f, 5e, 5f, 5g, 5h, 8a, 8band 8c):

Dolomitization has become widely recognized in many carbonate rocks of Kareem and Rudeis formations. In the studied carbonates, it is likely that there were three possible sources of Mg required for dolomitization. The most probably sources of Mg are that it was extracted from the overlying and underlying clay minerals from the shale intercalations in different rock units (Rudeis, Kareem, Esna, Matulla, Raha, Rod El Hamal and Abu Durba formations) by the effects of compaction and stress. Sea water, it is well known that during sea-level fall meteoric water could invade sea water forming mixing zone. The less effective source was the Mg derived by dissolution of skeletal grains originally composed of high-Mg calcite (calcareous algae, some foraminifers and echinoderms).

In the studied samples, dolomitization processes is the second phase where the dolomite rhombs were found to replace the recrystallized microsparite and sparry calcite. This means that dolomite replaced the neomorphic calcite after the recrystallization process.

The evenness of the crystal sizes, together with some large and well formed crystals produced by extensive dolomitization indicate that dolomitization occurred late during diagenesis. Dolomitization in the studied samples had almost completely replaced both the grains and matrix. This process normally occurs deep in the subsurface where all crystals have enough time to grow and form euhedral texture.

Genesis and models of dolomitization

Dolomitization process is one of the most important diagenetic processes acting on carbonate rocks. This process is very interested not only from natural scientific curiosity but also from the fact that many dolomite forms in nature have observed to be of considerable economic importance as hydrocarbon reservoirs (Zenger et al., 1980). The origin of dolomite could be known from observation of the preserved original limestone fabric and also from having a good idea about the depositional environment of the original carbonate (Bird and Jordan, 1977).

Several models for dolomitization of the carbonate rocks were proposed by many authors. These include the evaporative pumping model; the mixing zone model; the seepage reflux model; the seawater model and burial model.

Evaporative pumping model

The evaporative/ sabkha model was considered as the most plausible explanation for most examples of dolomitization for about 10 years after its popularization in dolomitization and limestone diagenesis (Pray and Murray, 1965).

In the sabkha model, progressive evaporation of marine and continental water derives sabkha pore fluids to gypsum saturation and lead to the precipitation of aragonite and gypsum with lagoon-derived aragonitic sabkha mud (Mckenzie et al., 1980). This precipitation causes a dramatic increase in the Mg/Ca ratio of the pore fluids from marine value of 5:1 to over 35:1. These elevated Mg/Ca ratio is suitable for the formation of dolomite, either by replacement of aragonitic sabkha mud or as a direct interstitial precipitation (Mckenzie, 1981).

The interpretation of dolomites of the Kareem and Rudeis formations are belonging to the sabkha environment is based on petrographical investigation, the crystal size tend to be small (but may gain significant sizes during later diagenesis), the absence of fluid inclusion, the association with gypsum and anhydrite and the presence of some scattered detrital quartz crystals (criteria characteristic to evaporitic model are after Moore et al., 1988).

Dedolomitization (Figs. 4a, 4bc, 4c and 4c):

Petrographic study of the Kareem and Rudeis formations shows an evidence of the presence of dedolomitization phenomenon in the dolomitic limestones. The evidence for dedolomitization is revealed by the common development of rhombohedral pores lined with fine calcite microspar representing remnant of un-dissolved dolomite grains which is considered as an indirect evidence for dedolomitization in dolomitic limestone. Dedolomitization thus seems to have partially reproduced the original texture of limestone.

Pressure solution (Figs. 5j, 5k, 7cand 7d):

This is indicated by the presence of stylolites. Stylolite is attributed to the pressure solution as a result of the overburden or tectonic pressure (Wanless, 1979).

Dissolution (Figs. 5l, 12e, 12f, 12gand 12h):

Dissolution versus precipitation processes plays the most important role in porosity evaluation. This lead to better understanding and evaluation of the reservoir quality of the studied Miocene rocks. Aragonitic bioclastic of coral, mulluscan shell algal remains suffered a partial and / or complete dissolution

in the surface zone leaving many biomoldic cavities. Patches dissolution of dolomite and anhydrite crystals developed vuggs and intercrystalline pores which produce a significant permeability of the dolostone rocks.

Fillings (Figs. 5d, 5f, 8a, 8band 8c):

The developed fractures and vuggs were filled by anhydrite, calcite and bituminous materials which reduce accordingly the available pore space. The source of the anhydrite can be attributed to the downward movement of $CaSO_4$ charged pore waters from the overlying evaporates (Gemsa, South Gharib and Zeit formations).

Anhydritization: anhydrite ($CaSO_4$) and gypsum ($CaSO_4.2H_2O$) are common minerals in dolostones reservoirs. Most of the gypsum changed to anhydrite; so we interpret the anhydrite cements in here. Distribution of anhydritic cements in Kareem and Rudeis formations is very much and have destructed the quality of reservoir on parts of the section. Anhydrite present in most of the facies and has filed pores such as interparticle, intercrystalline and moldic pores. The time of form of the anhydrite had widespread and we can observe primary to burial original anhydrite through the section. Anhydrite fabrics are poikilotopic and pore-Filling, Single and sporadic crystals anhydrite. From these fabrics, poikilotopic and pore filling anhydrite are the most common form of anhydrite in the par of dolostone in our studding reservoir.

Reservoir quality

The petrophysical properties such as total and effective porosity, permeability, pore size and distribution are substantially affected by diagenesis type and intensity. Thus, as emphasized by many authors (e.g., Rahimpour-Bonab, 2007), carbonates reservoirs which are prone to intense diagenetic alterations, could be compartmentalized (segmented) and represent variable petrophysical properties, even in small scales. So, a procedure for the identification and characterization of comparable diagenetic units from a petrophysical point of view would be useful to resolve some of the key challenges faced in the exploration and production of carbonate reservoirs.

The important feature relevant to reservoir prediction is the occurrence of high porosities in a wide range of microfacies types. This indicates that reservoir grade porosity development is not dependent upon the presence of any one depositional setting, but can be expected more or less throughout this interval. This statement should not be misconstrued as implying that porosity is not dependent upon depositional setting; rather, different combinations of porosity-favourable factors exist in different facies.

Reservoir quality improvement mainly controlled by diagenetic events. Two main diagenetic events are to encourage the improvement of reservoir quality, are dissolution and dolomitization. Dissolution has generated secondary porosity such vuggular and dolomitization which create micro-inter-crystalline porosity.

As a rule of thumb, in carbonate units by progress in the diagenetic processes and so overprints, pore types evolve imparting changes in petrophysical properties. The Kareem and Rudeis reservoir has porosity about 25%, it is considered as very good reservoir unit depending on the degree of the post – sedimentation diagenetic processes.

Conclusions

The petrographic investigation highlighted the main mineral components, textural aspects, diagenetic features and pore types geometry of the studied carbonate samples. Eight major microfacies types are recognized.

Dissolution, dolomitization and dedolomitization are the main diagenetic feature which create secondary porosity such moldic and vuggular, and intr-intra crystalline. The Kareem and Rudeis reservoir is graded from good to very good quality depending on the degree of the post – sedimentation diagenetic processes.

References
1. Abd El-Naby, A., Ghanem, H., Boukhary, M., Abd El-Aal, M. Lüning, S. and Kuss, J. 2010: Sequence stratigraphic interpretation of structurally controlled deposition: Middle Miocene Kareem Formation, Southwestern Gulf of Suez, Egypt: Geo Arabia., 15(3): 129-150.
2. Abdel Gawad, M. 1970: The Gulf of Suez: A brief review of stratigraphy and structure. Phil. Trans. Roy. Soc. London. A. 267, 41-48.
3. Abdel-Hafez, N. A. 1987: Evaluation of petroleum prospects of some areas in the Gulf of Suez region. A.R.E. Ph. D. thesis, El-Azhar Uni. Egypt., 527p.
4. Alsharhan, A. S. and Salah, M. G. 1997: The Miocene Kareem Formation in the southern Gulf of Suez, Egypt: a review on stratigraphy and petroleum geology: Journal of Petroleum Geology, 20(3): 327-346.
5. Amgad, S. S. 2011: Depositional model and diagenesis of the Miocene reef belt, Belayim Bay, Gulf of Suez, Egypt. M. Sc. thesis, Alexandria Uni. Egypt., 102 p.
6. Balduzzi, A., Cavaliere, R., Grignani, D., Lanzoni, E., Palmieri, G. and Rizzini, A. 1978: Stratigraphic and geochemical section Mediterranean Sea–Nile Delta–Gulf of Suez. Attivita Minerarie Servizio Studi Geologci E Laboratori, 1–23.
7. Baron D., Negrini, R. M, Golob E.M., Miller D., Sarna-Wojcicki A, Fleck R., Hacker B. and Erendi A. 2008: Geochemical correlation and 40Ar/39Ar dating of the Kern

River Ash and related tephra: Implications for the stratigraphy of petroleum-bearing formations in the San Joaquin Valley, California. Quaternary International, 176: 246-260.

8. Bird, H. K. and Jordan, C. F. 1977: Lisburne Group (Mississippian and Pennsylvanian), potential major hydrocarbon objective of Arctic. Slop, Alaska; Am. Assoc. Petrol. Geol. Bull., 61: 1493-1512.

9. Cerepi, A., Barde, J. P., Labat, N. 2003: High-resolution characterization and integrated study of a reservoir formation: the Danian carbonate platform in the Aquitaine Basin (France). Mar. Pet. Geol., 20: 1161–1183.

10. Chenet, P. Y. and Letouzey, J. 1983: Tectonique de la zone comprise entre Abu Durhaet Gebel Nezzazat (Sinai, Egypte) dans le contexte de levolution du rift de Suez. Bull. Centre Rec. Explo. Prod. Elf-Aquitaine, 7 (1): 201-215.

11. Choquette, P. W., and Pray, L. C. 1970: Geologic nomenclature and classification of porosity in sedimentary carbonates: Am. Assoc. Petrol. Geol. Bull. 54: 207-250.

12. Dunham, R. J. 1962: Classification of carbonate rocks according to depositional texture. In : Classification of carbonate rocks (Ed. By W. E. Ham), American Association of Petroleum Geology, 1 108– 121.

13. Egyptian General Petroleum Corporation, EGPC, 1964: Oligocene and Miocene rock- stratigraphy of the Gulf of Suez region, report of the Stratigraphic Committee: Egyptian General Petroleum Corporation, 142 pp.

14. EL-Albani, A., Vachard, D., Kuhnt, and Tnurow, J. 2001: Diagenetic carbonate concretion in the preservation of the original sedimentary rocks. Sed. Bull. 48: 875- 886.

15. El Beialy, S., Y., and Ali S. A. 2002. Dinoflagellates from the Miocene Rudeis and Kareem formations borehole GS-78-1, Gulf of Suez, Egypt. Journal of African Earth Sciences 35 (2002) 235–245.

16. El Beialy, S. Y., Mahmoud M. S. and Ali, A. S. 2005: Insights on the age, climate and depositional environments of the Rudeis and Kareem formations, GS-78-1 well, Gulf of Suez, Egypt: A Palynological Approach revista Española de Micropaleontología., 37(2): 273-289.

17. Fichera, R., Giori, I. and Milad, G. 1992: Southern Gulf of Suez; Interpretation of seismic, gravity and magnetic data as constraints in the resolution of deep structural setting. 11th EGPC Exploration Seminar, Cairo 1:31-44.

18. Folk, R. L. 1962: Spectral subdivision of limestone types." In. HAMED, W. E. (Ed): Classification of carbonate rocks: A. A. P. G., Mem. 1: 62-84, Tulsa / Oklahoma.

19. Folk R. L. 1974: Petrography of sedimentary rocks." Notes, Hemphill publ. Eo., Drawer M. Univ. station, Austin Texas, 174 pp.

20. Gandino, A., Giori, I. and Milad, G. 1990: Magnetic interpretation controlled by interactive 3D modeling in the southern Gulf of Suez: 10th Egyptian General Petroleum Corporation, Petroleum Exploration and Production Conference, 1: 740–786.

21. Gawad, W. A., Gaafar, I., Sabour, A. A. 1986: Miocene stratigraphic nomenclature in the Gulf of Suez region. In: Egyptian General Petroleum Corporation, 8th Exploration Conference, p. 1–20.

22. Khaled, M. A., Saber, M. S., Samir A. A. and Abd El-Azim E. 2009: Reservoir Characterization and Management, Role and Contribution in Improving Hydrocarbon Productivity Zeit Bay Field – Gulf of Suez, Egypt. AAPG European Region Annual Conference, Paris-Malmaison, France, 23-24 November, P. 437-462.

23. Mckenzie, J. A. 1981: Holocene dolomitization of calcium carbonate sediments from the coastal sabkha of Abu Dhabi, U.A.E. a stable isotope study. J. Geol. 89: 185-198.

24. Mckenzie, J. A., Hsu, K. J. and Schneider, J. F. 1980: Movement of subsurface waters under the sabkha. Abu Dhabi U.A.E and its relation to evaporation dolomite genesis in: Zenger, D. H. Dunham, J. B. and Ethington, R. L. (eds.) Concepts and models of dolomitization. SEPM spec. pub., 28: 1-30.

25. Meshrif, W. 1990: Tectonic framework of Egypt: In the Geology of Egypt, Edt. By Said, R., Balkima/Rotterdam/Brookfield, 113-155.

26. Moore, C. H., Chowdhury A., and Chan L. S. 1988: Upper Jurassic smack over platform dolomitization, Northwestern Gulf of Mexico In: V. Shukla and P. A. Baker (eds.), Sedimentology and geochemistry of dolostones. SEPM Spec. pub. 43pp.

27. Moustafa, A. G. 1976: Block faulting in the Gulf of Suez. 5th EGPC Exploration Seminar, Cairo, 1, 19 pp.

28. Moustafa, A.R. (1997): Controls on the development and transfer zones: The Influence of basement structures and sedimentary thickness in the Gulf of Suez and Red Sea. Jour. Structural Geology, 19, 755-768.

29. Peter, A. S. and Dana S. U. S. 2003: A Color Guide to the Petrography of Carbonate Rocks: Grains, textures, porosity, diagenesis. The Am. Assoc. Petrol.Geol. Tulsa, Oklahoma, U.S.A.

30. Pray, L. C. and Murray, R. C. 1965: Dolomitization and limestone diagenesis a symposium SEPM. spec. Publ. 13: 1-180.

31. Rahimpour-Bonab, H. 2007: A procedure for appraisal of a hydrocarbon reservoir continuity and quantification of its heterogeneity. Journal of Petroleum Science and Engineering, 58 (1): 1-12.

32. Rapson- McGaugan, J. E. 1970: The diagenesis and depositional environment of Permian ranger Canyon and Mowitch formations, Ishbel Group, from the Southern Canada Rocky Mountains. In H. Fuchtbauer (Ed.) Lithification of clastic sediments, 2 special issues, Sedimentology 15 (3/4): 205- 441.

33. Roehl, P.O. and Choquette, P. W. 1986: Carbonate petroleum reservoirs. Springer- Verlag, New York, 622 pp.

34. Said, R. 1962: The Geology of Egypt. Amsterdam: Elsevier.

35. Said, R. 1990: The Geology of Egypt. Rotterdam: Balkema.

36. Samir, M. Z. 2012: Provenance, diagenesis, tectonic setting and geochemistry of Rudeis Sandstone (Lower Miocene), Warda Field, Gulf of Suez, Egypt. Journal of African Earth Sciences 66-67: 56–71.

37. Stentoft, N., Lapinskas, P. and Musteikis, P. (2003): Diagenesis of Silurian reefal carbonates, Kudirka oilfield, Lithuania, Journal of Petroleum Geology, 26(4):381-402.

38. Tewfik, N., Harwood C. and Deighton, I. 1992: The Miocene, Rudeis and Kareem formations in the Gulf of Suez.: Aspects of sedimentology and geohistory: 11th EGPC Exploration Seminar, Cairo, 1: 84-113.

39. Tucker, M. E. 1981: Sedimentary petrology, an introduction. Blackwell Scientific Publication, Oxford, London, 252 pp.

40. Tucker, M. E. and Bathurst R. G. C. 1990: Carbonate diagenesis. Reprint Series 1, International Association of Sedimentology, Blackwell Scientific Publ. Oxford, 312 pp.

41. Wanless, H. R. 1979: Limestone response to stress: Pressure solution and dolomitization. Jour. Sed. Petrol., 49: 437-462.

42. Zenger, D. H., Dunham J. B. and Ethington R. L. 1980: Concepts and models of dolomitization. SEPM Special Publ. no. 28: 426 pp.

12/25/2015